A Biped Pattern Generation Allowing Immediate Modification of Foot Placement in Real-time

Mitsuharu Morisawa, Kensuke Harada, Shuuji Kajita, Kenji Kaneko,
Fumio Kanehiro, Kiyoshi Fujiwara, Shinichiro Nakaoka, Hirohisa Hirukawa
National Institute of Advanced Industrial Science and Technology(AIST)
1-1-1 Umezono, Tsukuba, Ibaraki, 305-8568, Japan
Email:{m.morisawa, kensuke.harada, s.kajita, k.kaneko,
f-kanehiro, k-fujiwara, s.nakaoka, hiro.hirukawa}@aist.go.jp

***Abstract*— This paper proposes a method of a real-time gait planning for biped robots which can change stride immediately at every step. Based on an analytical solution of an inverted pendulum model, the trajectories of COG (Center of Gravity) and ZMP (Zero-Moment Point) are parameterized by polynomials. Since their coefficients can be efficiently computed with given boundary conditions, this framework can provide a real-time walking pattern generator for biped robots. To handle the unexpected result caused by immediate changes of foot placement, we made single support periods as an additional trajectory parameter. The effectiveness of our method is shown by simulations of the humanoid robot HRP-2.**

I. Introduction

Humanoid robots are expected to contribute to the aging society with fewer children in the near future as labors. They have an advantage in working in an environment which are designed for human being. Thus, the human-size humanoid robots have been actively developing in the world [1]-[5]. To work in a human living, robots should have a walking ability as well as human's. Namely an ability of quickness will be requested to the robots for a working in a human living. Thus, how to change a landing position immediately is an important issue for a biped gait planning shown in Fig.1.

In order to generate a biped walking pattern in real-time, an inverted pendulum model which represents a dynamic behavior of the COG of the humanoid robot has been used [6]-[9]. When a landing position corresponds to a support point of an inverted pendulum, two steps are needed to change the desired landing position at least. Kagami *et al.*[6] realize a fast generation of dynamically stable humanoid robot walking pattern by discretizing the differential equation. The boundary condition of the COG can not be satisfied in this method. Takanishi et al. [3] proposed a method for generating the trunk motion of a humanoid robot by transforming the trajectory of the ZMP into the fourier series. Kajita *et al.*[7] proposed the generation method of biped walking pattern by using preview control. In this method, only after preview time, the landing position can be changed. Harada *et al.*[8] generated a real-time biped gait using an analytical solution. The connection of two trajectories is discussed in case of modification of next landing position. The generated biped pattern causes a curvature in case of connecting the trajectories in double support phase. Sugihara *et al.*[9] generated a biped walking

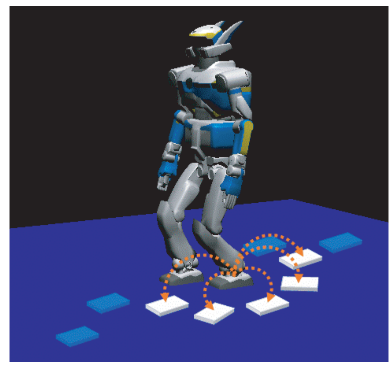

Fig. 1. Real-time gait planning

pattern every one step in real-time by relaxing the boundary condition of the ZMP. A generation system of a dynamically stable humanoid walking pattern which can updates at a short cycle was proposed by Nishiwaki *et al.*[16].

In this paper, a real-time gait planning method based on analytical solution of an inverted pendulum [8] which the COG and the ZMP trajectories are parameterized by polynomials. The both trajectories are generated simultaneously so that their coefficients can be satisfied the given boundary conditions are shown in sec. II. Section III shows a problem of a sequentially biped gait planning at every one step. In order to generate walking pattern more stably when the next landing position is modified, how to reshape the COG and the ZMP trajectories are shown in sec. IV. Section V presents the simulation results which show the effectiveness of our proposed method.

II. Simultaneous planning of COG and ZMP

The previous on-line modification of gait pattern could change only little landing position or was difficult to connect the ZMP trajectories continuously. In this paper, a biped gait is divided into the m-th sections every single or double support phase and each section is represented by applying an analytical solution of a linear inverted pendulum in addition to the ZMP polynomial which is proposed by Harada *at et*[8].

Firstly, $\boldsymbol{x}_G^{(j)} = [x^{(j)}\ y^{(j)}\ z^{(j)}]^T$ and $\boldsymbol{p}^{(j)} = [p_x^{(j)}\ p_y^{(j)}\ p_z^{(j)}]^T$ denote the COG and the ZMP position belonging to the j-th section. Let us focus on the COG motion on sagittal

1-4244-0200-X/06/$20.00

plane, and an dynamic equation of the COG in x-axis can be approximated by an inverted pendulum with a constant height ($z^{(j)} - p_z^{(j)} = \text{const.}$) which is given as follows:

$$\ddot{x}^{(j)} = \frac{g}{z^{(j)} - p_z^{(j)}}(x^{(j)} - p_x^{(j)}), \tag{1}$$

where g is gravity constant. The COG motion on lateral plane can be also formulated as the same equation. At j-th section, let us assume that the ZMP $p_x^{(j)}$ can be represented by N_j-th order time polynomial, that is

$$\begin{aligned} p_x^{(j)}(t) &= \sum_{i=0}^{N_j} a_i^{(j)} (\Delta t_j)^i, \\ \Delta t_j &\equiv t - T_{j-1}. \end{aligned} \tag{2}$$

Where, T_{j-1} implies the beginning time of j-th section. Substituting eq.(2) into eq.(1), the COG position $x^{(j)}$ can be solved.

$$x^{(j)} = V^{(j)} \mathrm{c}_j + W^{(j)} \mathrm{s}_j + \sum_{i=0}^{N_j} A_i^{(j)} (\Delta t_j)^i, \tag{3}$$

$$j = 1, \ldots, m,$$

$$A_i^{(j)} = \begin{cases} a_i^{(j)} + \displaystyle\sum_{k=1}^{(N_j - i)/2} b_{i+2k}^{(j)} \, a_{i+2k}^{(j)} \\ \qquad (i = 0, \ldots, N_j - 2) \\ a_i^{(j)} \quad (i = N_j - 1, N_j) \end{cases}$$

$$b_{i+2k}^{(j)} = \prod_{l=1}^{k} \frac{(i+2l)(i+2l-1)}{\omega_j^2}$$

Where, $\mathrm{c}_j \equiv \cosh(\omega_j \Delta t_j)$, $\mathrm{s}_j \equiv \sinh(\omega_j \Delta t_j)$, and $\omega_j \equiv \sqrt{g/(z^{(j)} - p_z^{(j)})}$. $V^{(j)}$ and $W^{(j)}$ denote the scalar coefficients. In previous research, the coefficients of the ZMP polynomial were set as unknown constants in the first section of double support phase. On the other hand, all of those are generalized as unknown constants. Thus, $2m + \sum_{j=1}^{m}(N_j + 1)$ number of unknown constants exist in eq.(3) during m-th section. To solve the biped gait planning as two point boundary value problem, the boundary conditions concerned with the COG and the ZMP are given as follows:

(I) Initial condition for the COG position and velocity:

$$x^{(1)}(T_0) = V^{(1)} + A_0^{(1)} \tag{4}$$

$$\dot{x}^{(1)}(T_0) = W^{(1)} + A_1^{(1)} \tag{5}$$

(II) Connection of two sections for the COG position and velocity

$$V^{(j)} \cosh(\omega_j \Delta T_j) + W^{(j)} \sinh(\omega_j \Delta T_j) + \sum_{i=0}^{N_j} A_i^{(j)} (\Delta T_j)^i = V^{(j+1)} + A_0^{(j+1)} \tag{6}$$

$$V^{(j)} \omega_j \sinh(\omega_j \Delta T_j) + W^{(j)} \omega_j \cosh(\omega_j \Delta T_j) + \sum_{i=1}^{N_j} i A_i^{(j)} (\Delta T_j)^{i-1} = W^{(j+1)} \omega_j + A_1^{(j+1)} \tag{7}$$

$$j = 1, \ldots, m-1$$

(III) Terminal condition for the COG position and velocity:

$$x^{(m)}(T_m) = V^{(m)} \cosh(\omega_m \Delta T_m) + W^{(m)} \sinh(\omega_m \Delta T_m) + \sum_{i=0}^{N_m} A_i^{(m)} (\Delta T_m)^i \tag{8}$$

$$\dot{x}^{(m)}(T_m) = V^{(m)} \omega_m \sinh(\omega_m \Delta T_m) + W^{(m)} \omega_m \cosh(\omega_m \Delta T_m) + \sum_{i=1}^{N_m} i A_i^{(m)} (\Delta T_m)^{i-1} \tag{9}$$

(IV) Initial condition for the ZMP position and velocity at each section:

$$p^{(j)}(T_{j-1}) = A_0^{(j)} - \frac{1}{\omega_j^2} A_2^{(j)} \tag{10}$$

$$\dot{p}^{(j)}(T_{j-1}) = A_1^{(j)} - \frac{6}{\omega_j^2} A_3^{(j)} \tag{11}$$

$$j = 1, \ldots, m$$

(V) Terminal condition for the ZMP position and velocity at each section:

$$p^{(j)}(T_j) = \sum_{i=0}^{N_j} \left\{ \left(A_i^{(j)} - \frac{(i+1)(i+2)}{\omega_j^2} A_{i+2}^{(j)} \right) (\Delta T_j)^i \right\} \tag{12}$$

$$\dot{p}^{(j)}(T_j) = \sum_{i=1}^{N_j} \left\{ i \left(A_i^{(j)} - \frac{(i+1)(i+2)}{\omega_j^2} A_{i+2}^{(j)} \right) (\Delta T_j)^{i-1} \right\} \tag{13}$$

$$j = 1, \ldots, m$$

where, $\Delta T_j \equiv T_j - T_{j-1}$. From the boundary condition (I)-(V), the total number of conditions becomes $6m + 2$. Then, all of unknown constants can be calculated by

$$\boldsymbol{y} = \boldsymbol{Z}^{+} \boldsymbol{w}, \tag{14}$$

where,

$$\boldsymbol{y} = \begin{bmatrix} V^{(1)} & W^{(1)} & A_0^{(1)} & \ldots & A_{N_1}^{(1)} & \ldots & V^{(m)} & W^{(m)} & A_0^{(m)} & \ldots & A_{N_m}^{(m)} \end{bmatrix}^T,$$

$$\boldsymbol{w} = \begin{bmatrix} x^{(1)}(T_0) & \dot{x}^{(1)}(T_0) & p^{(1)}(T_0) & \dot{p}^{(1)}(T_0) & p^{(1)}(T_1) & \dot{p}^{(1)}(T_1) & 0 & 0 & p^{(2)}(T_1) & \dot{p}^{(2)}(T_1) & \cdots & p^{(m)}(T_m) & \dot{p}^{(m)}(T_m) & x^{(m)}(T_m) & \dot{x}^{(m)}(T_m) \end{bmatrix}^T,$$

$$\boldsymbol{Z} = \begin{bmatrix} \boldsymbol{z}_{1,1} & \boldsymbol{0} & \ldots & \boldsymbol{0} & \ldots & \boldsymbol{0} \\ \boldsymbol{Z}_{2,1} & \boldsymbol{Z}_{1,2} & \boldsymbol{0} & & & \vdots \\ \boldsymbol{0} & \ddots & \ddots & \ddots & & \boldsymbol{0} \\ \vdots & \boldsymbol{0} & \boldsymbol{Z}_{2,j} & \boldsymbol{Z}_{1,j+1} & \boldsymbol{0} & \vdots \\ \boldsymbol{0} & & \ddots & \ddots & \ddots & \boldsymbol{0} \\ \vdots & & & \boldsymbol{0} & \boldsymbol{Z}_{2,m-1} & \boldsymbol{Z}_{1,m} \\ \boldsymbol{0} & \ldots & \boldsymbol{0} & \ldots & \boldsymbol{0} & \boldsymbol{z}_{2,m} \end{bmatrix},$$

$$
\begin{aligned}
\boldsymbol{Z}_{1,j} &= \begin{bmatrix} \mathbf{0}_{2\times N_j} \\ \boldsymbol{z}_{1,j} \end{bmatrix}, \boldsymbol{Z}_{2,j} = \begin{bmatrix} -\boldsymbol{z}_{2,j} \\ \mathbf{0}_{2\times N_j} \end{bmatrix}, \\
\boldsymbol{z}_{1,j} &= \begin{bmatrix} 1 & 0 & 1 & 0 & \frac{2}{\omega_j^2} & 0 & 0 & \dots & 0 \\ 0 & \omega_j & 0 & 1 & 0 & \frac{6}{\omega_j^2} & 0 & \dots & 0 \\ 0 & 0 & 1 & 0 & 0 & 0 & 0 & \dots & 0 \\ 0 & 0 & 0 & 1 & 0 & 0 & 0 & \dots & 0 \end{bmatrix}, \\
\boldsymbol{z}_{2,j} &= \left[\begin{matrix} 0 & 0 & 1 & \Delta T_j & (\Delta T_j)^2 \\ 0 & 0 & 0 & 1 & (\Delta T_j) \\ \mathrm{c}_j & \mathrm{s}_j & f_0^{(j)} & f_1^{(j)} & f_2^{(j)} \\ \omega_j \mathrm{s}_j & \omega_j \mathrm{c}_j & 0 & g_1^{(j)} & g_2^{(j)} \end{matrix} \right. \\
&\qquad \left. \begin{matrix} \dots & (\Delta T_j)^i & \dots & (\Delta T_j)^{N_j} \\ \dots & i(\Delta T_j)^{i-1} & \dots & N_j(\Delta T_j)^{N_j-1} \\ \dots & f_i^{(j)} & \dots & f_{N_j}^{(j)} \\ \dots & g_i^{(j)} & \dots & g_{N_j}^{(j)} \end{matrix} \right], \\
f_i^{(j)} &= \begin{cases} 1 & (i=0) \\ \Delta T_j & (i=1) \\ (\Delta T_j)^i - \frac{i(i-1)}{\omega_j^2}(\Delta T_j)^{i-2} & \\ & (i=2,\dots,N_j-2) \\ (\Delta T_j)^i & (i=N_j-1, N_j) \end{cases} \\
g_i^{(j)} &= \begin{cases} 1 & (i=1) \\ 2\Delta T_j & (i=2) \\ i(\Delta T_j)^{i-1} - \frac{i(i-1)(i-2)}{\omega_j^2}(\Delta T_j)^{i-3} & \\ & (i=3,\dots,N_j-2) \\ i(\Delta T_j)^{i-1} & (i=N_j-1, N_j) \end{cases} \\
& j = 1, \dots, m.
\end{aligned}
$$

Here, at least, the order of the ZMP polynomial N_j must satisfy

$$2m + \sum_{j=1}^{m}(N_j + 1) \geq 6m + 2. \tag{15}$$

III. Real-time continuous gait planning

In this section, we explain a method of real-time gait generation by re-planning walking pattern for each step and its problem. Figure 2 (a) illustrates the basic idea. At time T_0, the beginning of walking, we plan a walking pattern of two successive steps for the period of $[T_0 : T_5]$ as shown in the below graph of Fig.2 (a). We use the algorithm explained in the former section, which is fast enough to design two steps within one control cycle of 5[ms]. Since the planned walk will stop after two steps, we re-plan a walking pattern of the second and the third steps at time $T_2 (= T_0^{'})$ for the period of $[T_0^{'} : T_5^{'}]$ as shown in the above graph of Fig.2 (a). By repeating this for every step, a continuous walking can be generated.

Although this method seems to allow modification of stride for each step, it does not work as we expect. Let us explain this by using Fig.2 (b). In the below graph of Fig.2 (b), a walking pattern for two steps is planned at time T_0. Then at time $T_2 (= T_0^{'})$, we re-plan a pattern whose second step is smaller than previously designed. The resulting trajectory is shown in the above graph of Fig.2 (b). By the immediate change of the stride, the ZMP trajectory at single support period of $[T_0^{'} : T_2^{'}]$ had become convex shape. This is not an appropriate ZMP trajectory at single support phase, because a fluctuation of the ZMP is desired to be as small as possible so that it remains in a support polygon.

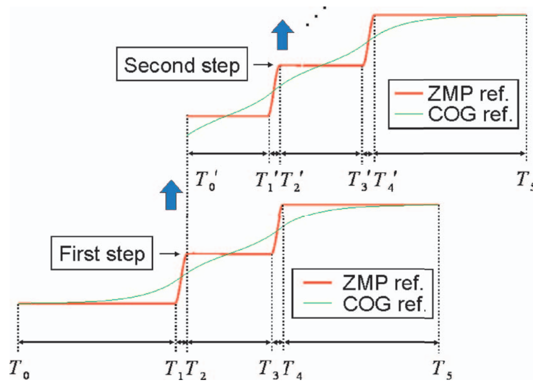

(a) Scheduled step

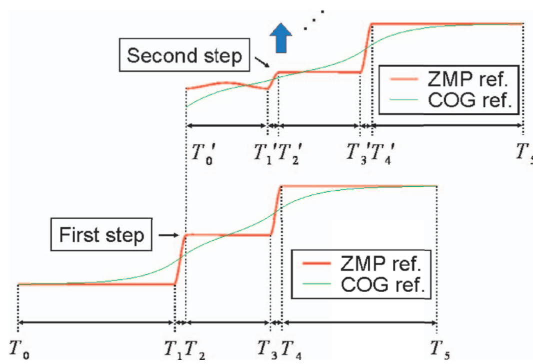

(b) Modified step

Fig. 2. Sequential gait planning

IV. Gait pattern compensation by immediate modification of foot placement

A. Time adjustment in single support phase

As mentioned above, the immediate modification of foot placement causes the fluctuation of the ZMP for the COG acceleration and deceleration. The variation value of the ZMP becomes large according to the modified length of stride. The COG can not be traced the desired trajectory unless the ZMP is generated within a support polygon. Thus, let us consider reducing the ZMP variation in single support phase by adjusting a period of single support phase. For example, because a curved ZMP trajectory forward than the desired it implies the deceleration of the COG velocity, an equivalent effect can be obtained by shortening a period of single support phase. On the other hand, in case of a backward ZMP fluctuation, it leads to make a period longer which is equivalent to slow down the COG motion.

Then, we explain how to determine an adjusting time of single support phase uniquely. Figure 3 (a) shows two preplanned gait patterns. One is that original COG trajectory is planned by 0.8[s] step cycle and 0.1[s] every step length. At the beginning of single support phase 4[s], a landing position will be modified from 0.4[m] to 0.6[m]. Other COG and ZMP trajectories will be generated on the assumption that the landing position was also preplanned in advance. Figure 3 (b) shows a zoom of Fig.3 (a) at about the time of the modification of foot placement. If it is possible for the COG state to transit from the original pattern to the modified pattern by shifting ΔT, the desired landing position can be realized without unnecessary ZMP variation.

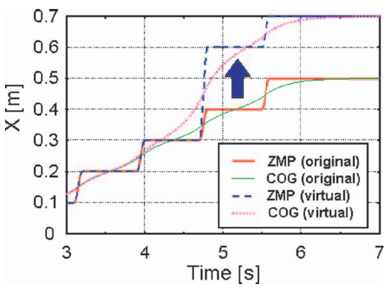

(a) COG and ZMP trajectories

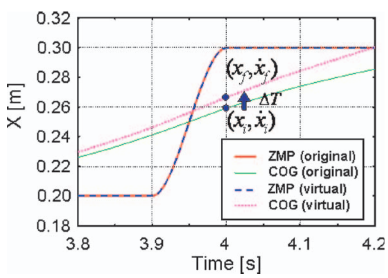

(b) Zoom up

Fig. 3. Compared with preplanned patterns

Here, let $x_i, \dot{x}_i$ and $p_i, \dot{p}_i$ be the COG position and velocity and the ZMP position and velocity at the original trajectory, and $x_f, \dot{x}_f$ and $p_f, \dot{p}_f$ be at the modified target one. The transition time can be calculated as

$$\Delta T = \begin{cases} \frac{1}{\omega}\log(r) & (r > 0) \\ \quad \text{s.t. } T_{\min} \le \Delta T \le T_{\max} & \\ T_{\max} & (r \le 0) \end{cases}, \quad (16)$$

$$r \equiv \frac{\omega(x_f^{'} - p_f^{'}) + (\dot{x}_f^{'} - \dot{p}_f^{'})}{\omega(x_i^{'} - p_i^{'}) + (\dot{x}_i^{'} - \dot{p}_i^{'})},$$

where ΔT should be used a value close to integral multiple at the control cycle. If the sum of the transition time and the period of single support phase is positive value, the ZMP trajectory is generated ideally. Since swing leg can not reach the target landing position in case of too short transition time, we set a lower limit of the transition time. When the transition time becomes too long at the large modification of stride, or can not be calculated at the change of walking direction, an enough time for single support will be given as maximum value.

Let us consider modifying next step length immediately from 0.1[m] to 0.3[m] at the beginning of single support phase

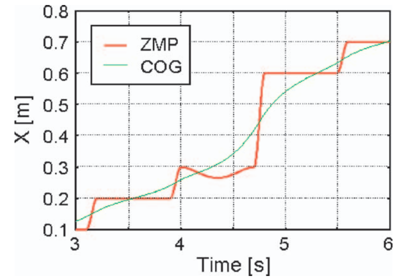

(a) Without time adjustment

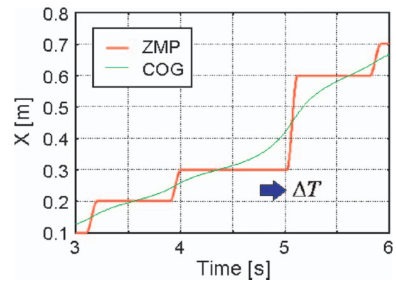

(b) With time adjustment

Fig. 4. Modification of foot placement

4[s] in Fig.4. The generated trajectory without time adjustment is shown in Fig.4 (a). In Fig.4 (a), the ZMP trajectory was fluctuated in the maximum backward by 26[mm]. Adding 0.31[s] to the period of single support phase, the maximum fluctuation of the ZMP was suppressed by up to 1[mm] shown in Fig.4 (b).

In this method, $x_i, \dot{x}_i$ and $x_f, \dot{x}_f$ can be obtained from matrix $\boldsymbol{Z}$ at a previous control cycle in eq.(14). After calculating an adjusting time, matrix $\boldsymbol{Z}$ will be obtained. Since matrix $\boldsymbol{Z}$ does not include any landing position and can be determined by the period of each support phase, the same matrix $\boldsymbol{Z}$ as on sagittal plane also can be utilized for the generation of the COG and the ZMP trajectories on lateral plane. Thus, the COG and the ZMP trajectories can be generated fastly by calculating a pseudo inverse matrix in eq.(14) only once at every control cycle.

B. Shaping of the ZMP trajectory

Although adjusting a single support period has effect to suppress the ZMP fluctuation in the motion direction, it in the orthogonal direction becomes large. The ZMP fluctuation will be canceled by the opposite phase. The opposite phase of the ZMP fluctuation can be generated by preview control [7]. By setting initial position and velocity of the COG to zeros, the COG and the ZMP trajectories can be connected to the originals smoothly. The block diagram of the ZMP shaping is shown in Fig.5. Figure 5 (a) implies that the ZMP trajectory had occurred the overshoot by the immediate modification of next foot placement at a beginning of single support. Then, the COG and the ZMP trajectories are generated so that the output ZMP can follow the unexpected ZMP fluctuation as the desired ZMP by preview control method in (b). Subtracting (b) from (a), newly reference trajectory of the ZMP can be obtained as (c). The reference trajectory of the COG can be also synthesized as well as the ZMP's. Especially, if the order of the ZMP polynomial at the first section is set to four, the peak time of the ZMP fluctuation becomes middle and the time to suppress the ZMP fluctuation can be acquired.

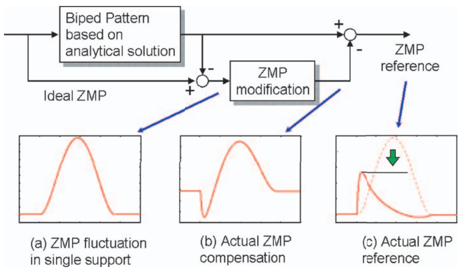

Fig. 5. Block diagram of the ZMP shaping

V. Simulation results

To confirm the effectiveness of the proposed method, some cases of the real-time gait planning without/with the immediate modification of stride will be compared, that is:

(a) Original pattern (predesigned stride)
(b) Stride modification
(c) Stride modification + Time adjustment
(d) Stride modification + ZMP shaping
(e) Stride modification + Time adjustment + ZMP shaping

The parameters of gait planning are shown in Table.I. Case (a) indicates the predesigned stride. The right allows means the immediate modification of foot placement at the beginning of single support phase in case (b)-(e). ΔT denotes the adjusting time at case (c) and (e) by eq.(16), where the maximum adjusting time is set to 0.8[s].

TABLE I
PARAMETERS FOR GAIT PLANNING

Original		Modification	
Time [s]	(a) [m]	ΔT [s]	(b)-(e) [m]
0	0.0	-	0.0
2.4	0.1	-	0.1
3.2	0.2	-0.175	0.2 $\rightarrow$ 0.1
4.0	0.3	-	0.3
4.8	0.0	0.8	0.0 $\rightarrow$ 0.3
5.6	-0.1	0.18	-0.1 $\rightarrow$ -0.2
6.4	-0.2	-	-0.2
7.2	-0.3	0.8	-0.3 $\rightarrow$ 0.3
8.0	0.0	0.8	0.0 $\rightarrow$ 0.3

In these simulations, the future three steps are used for the biped gait planning. Thus, the number of sections is seven ($m = 7$). At the initial and the terminal sections of the biped gait, the fourth order ZMP polynomials are applied ($N_1 = N_7 = 5$). The third order ZMP polynomials are used at the intermediate sections so that its coefficients can be determined uniquely to reduce the dimension of matrix $\boldsymbol{Z}$ in eq.(14). This implies that the ZMP coefficients of intermediate trajectories are directly calculated from the boundary conditions. As a result, the dimension of matrix $\boldsymbol{Z}$ can be reduced from 44 to 20. The total computation time including a time adjusting and the ZMP shaping became 0.9[ms] (Pentium III 1.26[GHz]).

The generated trajectories which are applied to the humanoid robot HRP-2[5] using a dynamic simulator OpenHRP [19] are shown in Fig.6 (a)-(e). No compensating the ZMP trajectory in case (b) causes a falling over is shown in Fig.7. In fig.6 (b) and (c), the ZMP trajectories get close to the edge of support polygon when the foot placement is modified from

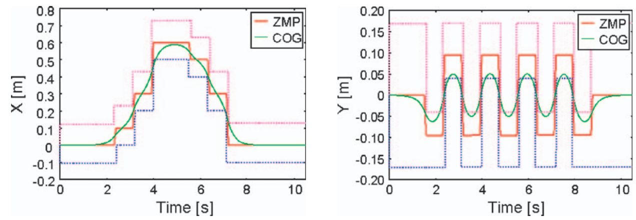

(a) Original pattern

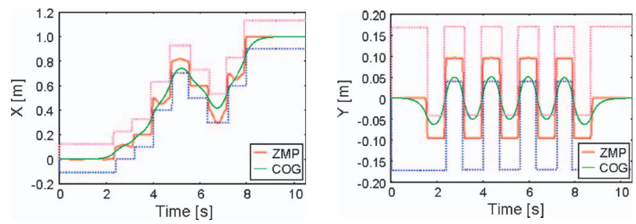

(b) Stride modification

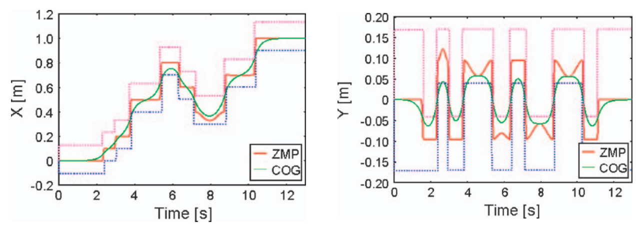

(c) Stride mod. + Time adjustment

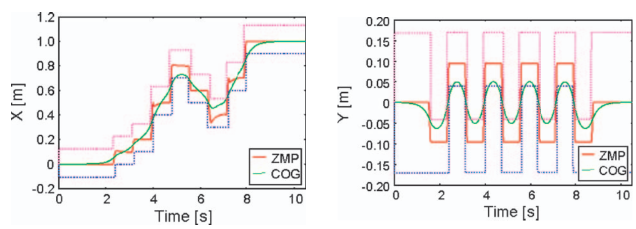

(d) Stride mod. + ZMP shaping.

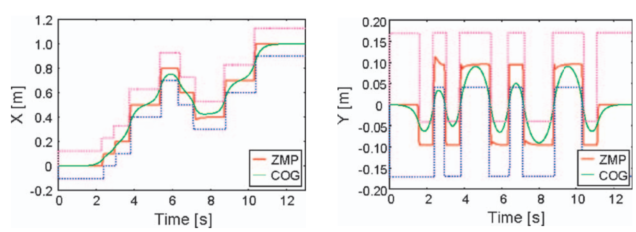

(e) Stride mod. + Time adj + ZMP shaping.

Fig. 6. Comparison of patterns

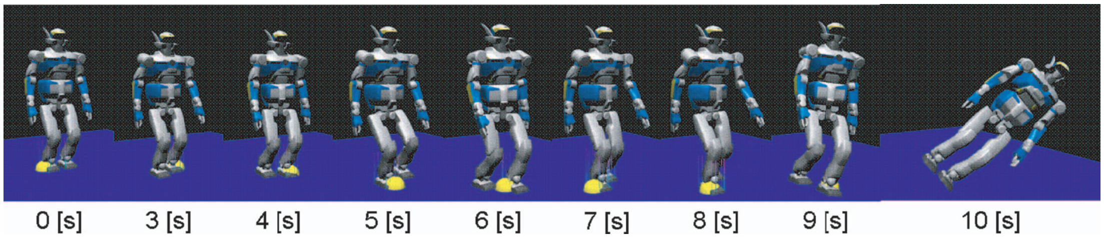

Fig. 7. Snapshot of the playbacked immediate modification of foot placement without any compensation (b)

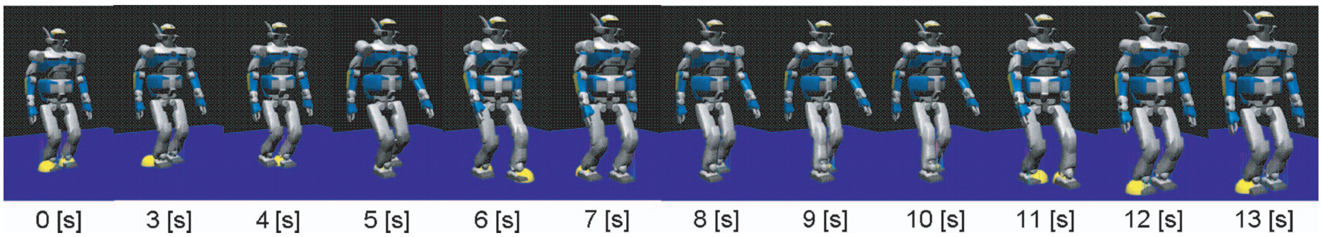

Fig. 8. Snapshot of the playbacked immediate modification of foot placement with time adjustment + ZMP shaping (e)

-0.3[m] to 0.3[m]. In these cases, it was difficult to walk stably. In cases of (d) and (e), it was possible to walk without a falling over. In case (e), we can see that there is the widest stability margin and the stable walking could be realized in spite of the large modification of foot placement immediately in Fig.8.

VI. CONCLUSION

This paper proposed a method of a real-time gait planning which can change stride immediately at every one step. Based on an analytical solution of an inverted pendulum, the COG and the ZMP trajectories which satisfy two point boundary value problem could be generated simultaneously by parameterizing the coefficients of the ZMP polynomials. A stable walking pattern could be generated smoothly by adjusting a period of a single support phase and shaping the ZMP fluctuation in spite of unexpected modification of the next step. The effectiveness of the proposed method was confirmed by the immediate modification of stride in simulations.

REFERENCES

[1] K.Hirai, et al., “The Development of Honda Humanoid Robot,” Proc. of IEEE Int. Conf. on Robotics and Automation, pp.1321-1326, 1998.
[2] M.Gienger, et al., “Towards the Design of Jogging Robot,” Proc. of IEEE Int. Conf. on Robotics and Automation, pp.4140-4145, 2001.
[3] H.Lim, Y.Kaneshima, A.Takanishi, et al., ”Online Walkinge Pattern Generation for Biped Humanoid Robot with Trunk,” Proc. of IEEE Int. Conf. on Robotics and Automation, pp.3111-pp.3116, 2002.
[4] J.Y.Kim, et al., “System Design and Dynamic Walking of Humanoid Robot KHR-2,” Proc. of IEEE Int. Conf. on Robotics and Automation, pp.1443-1448, 2005.
[5] K.Kaneko, et al., “The Humanoid Robot HRP2,” Proc. of IEEE Int. Conf. on Robotics and Automation, pp.1083-1090, 2004.
[6] S.Kagami, at el., “A Fast Generation Method of a Dynamically Stable Humanoid Robot Trajectory with Enhanced ZMP Constraint,” Proc. of the 2000 IEEE-RAS Int. Conf. Humanoid Robots, 2000.
[7] S.Kajita, et al., “Biped Walking Pattern Generation by using Preview Control of Zero-Moment Point,” Proc. of IEEE Int. Conf. on Robotics and Automation, pp.1620-1626, 2003.
[8] K.Harada, et al., “An Analytical Method on Real-time Gait Planning for a Humanoid Robot,” Proc. of the 2000 IEEE-RAS Int. Conf. Humanoid Robots, Paper #60, 2004.
[9] T.Sugihara, et al., “A Fast Online Gait Planning with Boundary Condition Relaxation for Humanoid Robot,” Proc. of IEEE Int. Conf. on Robotics and Automation, pp.306-311, 2005.
[10] K.Nagasaka, et al., “Integrated Motion Control for Walking, Jumping and Running on a Small Bipedal Entertainment Robot,” Proc. of IEEE Int. Conf. on Robotics and Automation, pp.3189-3194, 2004.
[11] M.Vukobratovic, and D.Juricic, “Contribution to the Synthiesis of Biped Gait,” IEEE Trans. on Bio-Med. Eng., vol.BME-16, no.1, pp.1-6,1969.
[12] H.Miura, et al., “Dynamic walk of a biped,” Int. Jour. of Robotics Research, Vol.3, No.2, pp.60-72, 1984
[13] K.Nishiwaki, et al., “Online Mixture and Connection of Basic Motions for Humanoid Walking Control by Footprint Specification,” Proc. of IEEE Int. Conf. on Robotics and Automation, pp.4110-4115, 2001.
[14] S.Kajita, et al., “The 3D Linear Inverted Pendulum Mode: A simple modeling for a biped walking pattern generation,” Proc. of IEEE/RSJ Int. Conf. on IROS, pp.239-246, 2001.
[15] T.Sugihara, et al., “Realtime Humanoid Motion Generation through ZMP Manipulation based on Inverted Pendulum Control,” Proc. of IEEE Int. Conf. on Robotics and Automation, pp.1404-1409, 2002.
[16] K.Nishiwaki, et al., “High Frequency Walking Pattern Generation based on Preview Control of ZMP,” Proc. of IEEE Int. Conf. on Robotics and Automation, pp.2667-2672, 2006.
[17] Ill-Woo Park, et al., “Online Free Walking Trajectory Generation for Biped Humanoid Robot KHR-3(HUBO),” Proc. of IEEE Int. Conf. on Robotics and Automation, pp.1231-1236, 2006
[18] S.Kajita, “Humanoid Robots”, Ohmusha, ISBN4-274-20058-2, 2005. (in Japanese)
[19] F.Kanehiro, et al., “Open Architecture Humanoid Robot Platform,” Proc. of IEEE Int. Conf. on Robotics and Automation, pp.24-30, 2002